Effects of perfluoroalkylsilane molecular assembly on flow induced voltage generated by doped silicon wafers

U. Satheesh, P. Prakash, and D. Devaprakasam

Citation: Journal of Applied Physics **121**, 025501 (2017); doi: 10.1063/1.4974003
View online: http://dx.doi.org/10.1063/1.4974003
View Table of Contents: http://aip.scitation.org/toc/jap/121/2
Published by the American Institute of Physics

Effects of perfluoroalkylsilane molecular assembly on flow induced voltage generated by doped silicon wafers

U. Satheesh,[1] P. Prakash,[1] and D. Devaprakasam[2,3,a)]
[1]*Department of Nanosciences and Technology, Karunya University, Coimbatore, Tamil Nadu 641114, India*
[2]*Department of Mechanical Engineering, School Mechanical and Building Sciences, VIT University, Chennai, Tamil Nadu, 600127, India*
[3]*InCUBE-EngSciRes R&D, Udumalpet, Coimbatore, Tamil Nadu 642126, India*

(Received 14 July 2016; accepted 31 December 2016; published online 12 January 2017)

We report the effects of surface modifications on (i) Seebeck coefficients and (ii) flow induced voltage generations of the n-type (n-Si) and p-type (p-Si) silicon wafers. The surfaces of n-Si and p-Si wafers were coated with 1H,1H,2H,2H- perfluorooctyltrichlorosilane (FOTS) molecules. The surface modified n-Si and p-Si of size 12 mm × 4 mm were mounted on the $\pi/4$ angle inclined experimental mount, and nitrogen gas was flown over the inclined surface at the subsonic velocities, 5.3, 10.61, 15.91, 21.22, and 26.52 ms^{-1}, and the voltage difference between the lead and rear ends of pristine and surface modified n-Si and p-Si was measured. The experimental results and theoretical relations are presented. The flow induced voltage generation is caused by the interplay between the Bernoulli flow and Seebeck effect. The flow-voltage response results show that the half coated and full coated n-Si and p-Si wafers generate more voltage than that of the uncoated at a given velocity. The band theory reveals that the flow of nitrogen gas accumulates charge carriers at the FOTS self assembled monolayer (SAM)—silicon interfaces, which resulted in the more voltage generation by full and half coated ni-Si and p-Si surfaces than that of the pristine surface. The enhanced voltage generations and high sensitivities are caused by an effective increase of the gradient of Fermi Energy (E_F) (Seebeck coefficient) due to FOTS SAM coatings. Because of that the FOTS SAM modified n-Si and p-Si are become highly sensitive to nitrogen gas flow. *Published by AIP Publishing.*
[http://dx.doi.org/10.1063/1.4974003]

I. INTRODUCTION

Short chain organosilanes are usually in the order of few nm,[1–5] and when they are self assembled on the solid surfaces, they modify the surface properties, optical properties, electronic properties, mechanical properties, and thermal properties of the native solid surfaces.[1–3,6–8] By using different methods like liquid phase[9] and vapor phase,[4,10–13] organosilane self assembled monolayers (SAMs) can be easily patterned on the Si wafers and other engineering surfaces. SAM modified solid surfaces are used as sensors and detectors and find applications in many fields of engineering and technology.[1,5,14] Self assembled monolayers of perfluoroalkylsilanes are highly hydrophobic and thermally stable on solid surfaces because of the order-disorder mechanisms of CF_2 and CF_3.[2] Synergism of the properties of the perfluoroalkylsilane SAM with solid surfaces produced very sensitive and highly active surfaces, which are successfully used in many engineering and technological applications.[6,15]

Highly doped silicons are used as thermo-electric devices and sensors in many engineering applications because of their high Seebeck coefficients.[14,16–19] Earlier literature studies report that the flow of fluids over the surfaces of heavily doped silicon, carbon nanotubes, graphene, and other doped semiconductors generates measurable amounts of voltage difference between the lead and rear ends.[20–30] It is observed that the magnitudes of the generated voltages are proportional to Seebeck coefficients (α_s) of the respective materials and the square of the differential flow velocity. When a steady flow of nitrogen gas passes over an inclined surface at $\pi/4$, the velocity difference between the lead end and the rear end of the solid surface produces a pressure difference due to Bernoulli flow and the pressure difference in turn gives rise to the temperature difference because of the incompressible characteristics of gases. This temperature difference produces a finite voltage difference due to the Seebeck effect.[21,22,31,32]

Our objective of the study is to understand the effect of FOTS SAM modification on the Seebeck coefficient and flow induced Seebeck voltage generations of n-Si and p-Si semiconductors and further investigate the flow sensitivities of the same for the nitrogen gas sensing applications. In this work, we designed and developed an experimental setup to measure nitrogen gas flow induced voltage generation and measured voltage generated by uncoated, half coated, and full coated n-Si and p-Si wafers. Based on the band theory, the effect of FOTS SAM coating on Seebeck coefficients and voltage generation due to nitrogen gas flow was analysed and discussed.

II. THEORY

A. Seebeck effect of the silicon-FOTS SAM

In bi-metal junctions, when the ends were kept at hot and cold temperatures, the valence electrons in the hot end

a)Author to whom correspondence should be addressed. Electronic mail: devaprakasam.d@vit.ac.in

have high kinetic energy and become more populated, and higher concentration electrons above the Fermi energy in the warmer part move towards the cold part, which results in a finite voltage difference between hot and cold ends, and this is known as the "Seebeck Effect." In semiconductors, the temperature gradient causes the gradient in the Fermi energy. According to the Fermi-Dirac distribution and band theory, when the temperature increases, the Fermi energy level moves towards the conduction band. The temperature difference between the hot and cold ends of the silicon causes a gradient in Fermi energy levels.[14,16–19] Therefore, the Seebeck coefficients of n-Si and p-Si are defined as the gradient of the Fermi energy E_F with respect to temperature

$$\frac{\Delta E_F}{q} = \alpha_s \Delta T \tag{1}$$

or

$$\alpha_s = \frac{1}{q}\frac{\mathrm{d}}{\mathrm{d}T}(E_F), \tag{2}$$

where the Fermi energy of n-Si is $E_F = E_c - kTln\left(\frac{N_c}{N_d}\right)$ and that of p-Si is $E_F = E_v + kTln\left(\frac{N_v}{N_a}\right)$.

As we know that for silicon the energy gap (E_g) is also function of temperature $E_g(T) = E_g(0) - (\frac{\alpha T^2}{T+\beta})$, where $E_g(0) = 1.166\,\mathrm{eV}$, experimental fit $\alpha = 4.73 \times 10^{-4}\,\mathrm{eV/K}$ and $\beta = 636\,\mathrm{K}$ Any change in temperature changes the absolute values of E_c and E_v and results in a change in the Fermi-Dirac distribution function. Hence, there are two contributions to Seebeck coefficient α_s, (i) change of $E_F - E_c$ and $E_F - E_v$ and (ii) change of absolute values of E_c and E_v. The temperature difference in the silicon causes a net flow of phonons from hot to cold. In a certain temperature region ($-10\,\mathrm{K}$ to $500\,\mathrm{K}$) and for non-degenerate silicon, a transfer of momentum from acoustic phonons to the charge carriers can occur. As there is a net phonon momentum directed from hot to cold, this would drag the charge carriers towards the cold side of the silicon. Taking account of all the contributions, the Seebeck coefficient of doped silicon is the sum of slope of E_F and internal electric field E which was induced by net diffusion currents and by phonon-drag currents. It can be expressed as, (i) for n-Si

$$\alpha_s = -\frac{k}{q}\left\{ln\frac{N_c}{N_d} + \frac{5}{2} + s_n + \phi_n\right\}. \tag{3}$$

(ii) for p-Si

$$\alpha_s = +\frac{k}{q}\left\{ln\frac{N_v}{N_a} + \frac{5}{2} + s_p + \phi_p\right\}, \tag{4}$$

where "s" is the exponent describing the relation between relaxation time and the charge-carrier energy and ϕ denotes the phonon drag effect. And the values of "s" are in the range of -1 to 2, and value of ϕ is zero for the highly doped semiconductor. It is reported that the Seebeck coefficient of silicon is a function of dopant concentration,[14] and simplified expressions for heavily doped silicon ($>10^{19}\mathrm{cm}^{-3}$) at room temperature are (i) for n-Si, $\alpha_s = -\frac{k}{q}(ln\frac{N_c}{N_d} + 4)$ and (ii) for p-Si, $\alpha_s = +\frac{k}{q}(ln\frac{N_v}{N_a} + 4)$ The Seebeck coefficient strongly depends on the impurity concentration, and both electrical and thermal conductivities have an influence on α_s[16–19,33] In practice, the Seebeck coefficient may be approximated in terms of electrical conductivity as a function of depth 'r' radial distance from the surface, proposed by Nieveld[14,16–19]

$$\alpha_s = \frac{mk}{q}\left(ln\frac{\sigma_0}{\sigma(r)}\right) \tag{5}$$

with $\sigma_0 = 3.1 \times 10^5\mathrm{S/m}$ and $m \approx 2$; it is found that the effective Seebeck coefficient is equal to the coefficient of the surface layer plus a correction factor dependent on the shape of the conductivity profile. The above empirical relation (5) can be expressed in terms of resistivity as a function of depth 'r' radial distance from the surface, $\alpha_s = \frac{mk}{q}(ln\frac{\rho(r)}{\rho_0})$ with $\rho_0 = 5 \times 10^{-6}\Omega - m$ and $m \approx 2.6$.

From Equation (5), it is very obvious that the self-assembly of the FOTS SAM changes both the electrical conductivity and thermal conductivity of the surface and subsurface. The silane groups of the FOTS molecules were chemically bonded to the surface of the n-Si and p-Si through oxygen and this would change the impurity concentration of n-Si and p-Si surfaces, which results in a change in values of both E_F and E_c. Moreover, FOTS molecules are high band gap semiconductors $(E_g = 3.8\ \mathrm{eV})$. Therefore, FOTS molecules on the n-Si and p-Si surfaces act as energy barriers to charge carriers. Therefore, the Seebeck coefficients (α_s) of the doped n-Si and p-Si are given by Equations (3) and (4).

B. Bernoulli's effect on the silicon-FOTS SAM

When steady flow nitrogen gas passes over the inclined surface of highly doped silicon, the tangential component of the velocity "u" of the outer flow depends on the streamline distance "x" measured along the flat boundary as

$$u(x) \propto u(0)x^{\frac{\theta}{(\pi-\theta)}}. \tag{6}$$

For $\theta = \pi/4$, then $u(x) \propto x^{\frac{1}{3}}$. The velocity difference ΔV between the lead and rear ends produces pressure gradient ΔP and the pressure difference produces a temperature difference (ΔT) due to the incompressible characteristics of gases $(\Delta P/P = \Delta T/T)$.[21,22,31,32] The nitrogen gas flow will induce a temperature difference in the solid along the flow direction. The temperature difference, in turn, will result in a voltage difference V, defined as $V_L - V_R$, due to the Seebeck effect. The voltage difference due to the flow of nitrogen gas is given in terms of velocities and is given by

$$\Delta V = 4\alpha_s k T_0(\gamma - 1)(\Delta u^2) \times 10^{-6}, \tag{7}$$

where $\gamma = 1.667$, $k = 1$, and $T_0 = 300\,\mathrm{K}$. Equation (7) can be simplified and rewritten as[21,22]

$$V = D_s u^2 \tag{8}$$

or

$$V = A_s M_n^2 \tag{9}$$

V is proportional to the square of the velocity u^2; it clearly indicates the linearity between V and u^2 and M_n^2, where M_n is the Mach number given by $M_n = \frac{u}{c}$, c being the sound velocity($c = 353\,\mathrm{ms}^{-1}$ for nitrogen at 300 K).

III. EXPERIMENTAL DETAILS

A. Materials details

The n-type silicon wafers of single side polished, ⟨100⟩, crystalline ($cubic(a = 5.4037)$), 0.5 mm thickness with phosphorus dopant concentration $\approx 1 - 3 \times 10^{18}\mathrm{cm}^{-3}$, resistivity $\rho \approx 0.01\,\Omega\,\mathrm{cm}$, and the Seebeck coefficient $\alpha_s \approx -450\,\mu\mathrm{V/C}$ and the p-type silicon wafers of single side polished, ⟨100⟩, crystalline ($cubic(a = 5.4037)$), 0.5 mm thickness with boron dopant concentration $\approx 1 - 3 \times 10^{18}\mathrm{cm}^{-3}$, resistivity $\rho \approx 0.0095\,\Omega\,\mathrm{cm}$, and Seebeck coefficient $\alpha_s \approx +450\,\mu\mathrm{V/C}$, were used. 1H,1H,2H,2H- perfluorooctyltrichlorosilane (FOTS) of 99.8% purity and Isooctane of 99% Purity were used. All the materials were purchased from Sigma Aldrich, USA.

B. Preparation of FOTS-SAM

1 mM of FOTS molecules were prepared in the isooctane solvent, and the solution was ultrasonicated for 15 min. The n-Si and p-Si wafers of size 12 mm × 4 mm were cut. The n-Si and p-Si wafers were immediately immersed/semi immersed in a freshly prepared solution for a duration of about 15 min.[3,15] We also prepared n-Si and p-Si samples, which were immersed/semi immersed for 2 and 18 h in the freshly prepared solution. After SAM deposition, the p-Si and n-Si wafers were taken out and stored in a desiccator. The FOTS SAM formation on the Si wafers is shown schematically in Fig. 1. The FOTS SAM coated p-Si and n-Si wafers were used as sensing elements in the flow measurements.

C. FTIR, EDAX, and AFM Measurements

The Surfaces of the FOTS SAM coated n-Si and p-Si wafers were characterized by Grazing angle FTIR, Energy Dispersive X-ray Analysis (EDAX), and AFM. The FTIR spectra were taken by a Perkin-Elmer GX2000 spectrometer at 4 cm^{-1} resolution for an optimized 512 scans with a liquid nitrogen-cooled MCT detector, and the spectra were collected by spectra software and a data acquisition system. The sample chamber and detector were purged with nitrogen gas before starting the experiment and at regular intervals. The sample stage has a fixed angle of incidence of 75°. Elemental analysis of FOTS SAM coated n-Si and p-Si wafers were investigated by an Oxford Instrument INCA Penta FXT X3 X-ray analyzer.

The surface morphology and topography of the FOTS SAM coated n-Si and p-Si wafers were characterized by Bruker Innova Atomic Force microscopy. The experiments were performed in the contact mode; the topography image was taken at a scan resolution of 512 × 512 and the scan area was approximately 1 μm × 1 μm.

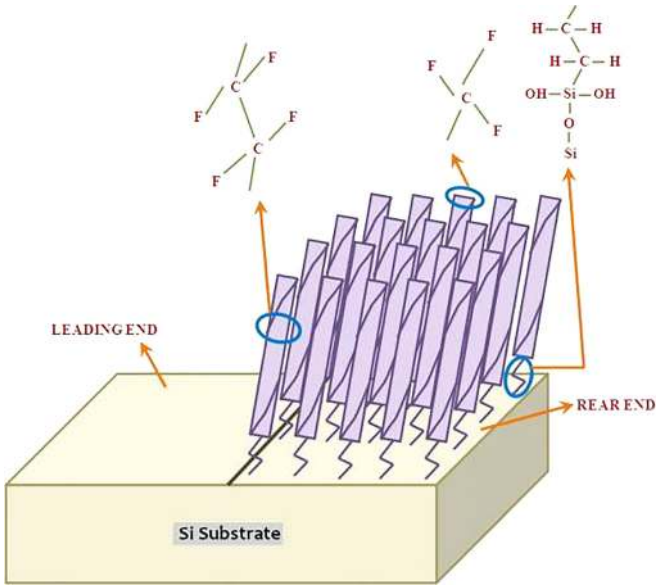

FIG. 1. Schematic of the half coated FOTS SAM on the surface of Si.

D. Experimental setup

The experimental setup shown in Fig. 2 consists of a flow duct (D), which is connected to a nitrogen gas cylinder. The flow rate is measured with the help of a flow meter (F). The sensor attached to an aluminum mount (M) is placed in front of the open end of the flow duct at an inclination of $\pi/4$. The FOTS SAM coated n-Si and p-Si wafers are attached over the aluminum mount. The sensing element was separated from the metal mount M with electrically and thermally insulating materials. The two copper connection leads are taken from the sensing materials using silver conductive paste, and then leads are connected to the National instruments NI-PXI-1044 Workstation. The mechanical valve was used to control the on and off flow of nitrogen gas at the interval of 1–2 s. The voltage response was measured continuously for a duration of 25 s at different flow velocities of 0.0, 5.3, 10.61, 15.91, 21.22, and 26.52 ms^{-1}.

IV. RESULTS AND DISCUSSION

A. Surface analysis

Fig. 3 shows the FTIR spectra of FOTS SAM on n-Si and p-Si surfaces. The CF_2 symmetric (ν_s) and asymmetric

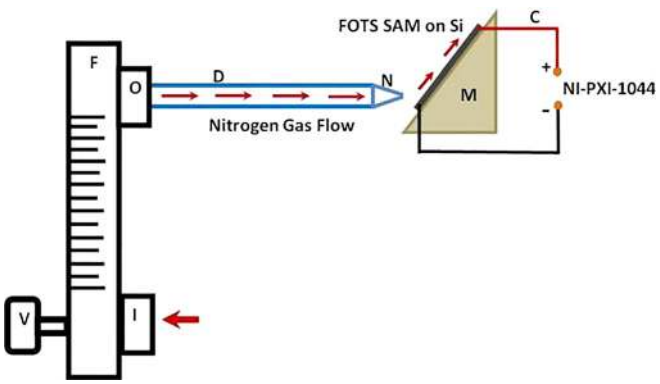

FIG. 2. Schematic of the flow induced measurement setup.

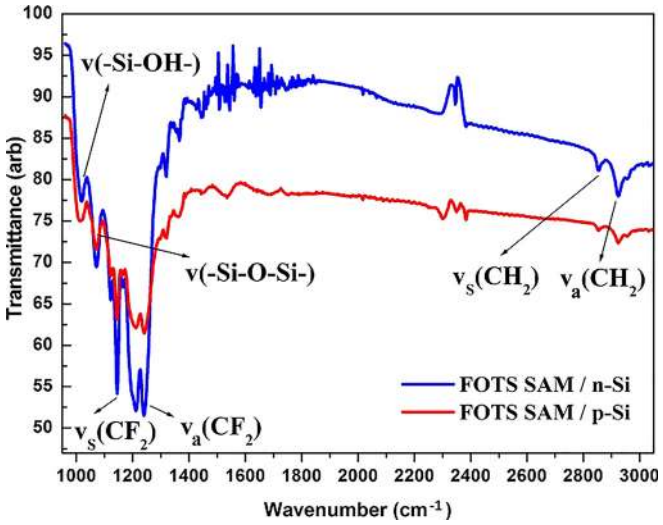

FIG. 3. FTIR Spectra of the FOTS SAM coated on n-Si and p-Si surfaces.

(ν_a) stretching vibrations for the n-Si surface are observed at $\nu_s = 1145$ cm^{-1} and $\nu_a = 1244$ cm^{-1}, respectively, and those for the p-Si surface are observed at the stretching vibrations at $\nu_s = 1151$ cm^{-1} and $\nu_a = 1248$ cm^{-1}, respectively. The vibration at 1076 cm^{-1} indicates the presence of unpolymerized silanol group Si-OH, and the degree of polymerization is low in the case of n-Si compared to p-Si. The stretching vibrations of the polymerized siloxane network $(-Si-O-Si-)$ for the n-Si surface are observed at 1020 cm^{-1} and for the p-Si surface are observed at 1005 cm^{-1}, respectively. The vibration at 1076 cm^{-1} indicates the presence of unpolymerized silanol group Si-OH, and the degree of polymerization is low in the case of n-Si compared to p-Si. From the observation, it is very clear that FOTS SAM molecules are more ordered on n-Si, and FOTS SAM molecules are more disordered on p-Si, indicated by the stretching vibrations and the degree of siloxane formation. The X-ray Elemental analysis of the FOTS SAM coated n-Si and p-Si surfaces is shown Fig. 4, and the presence of F, Si, and C elements was confirmed. The surface morphology and topography images were further investigated by AFM, and from the

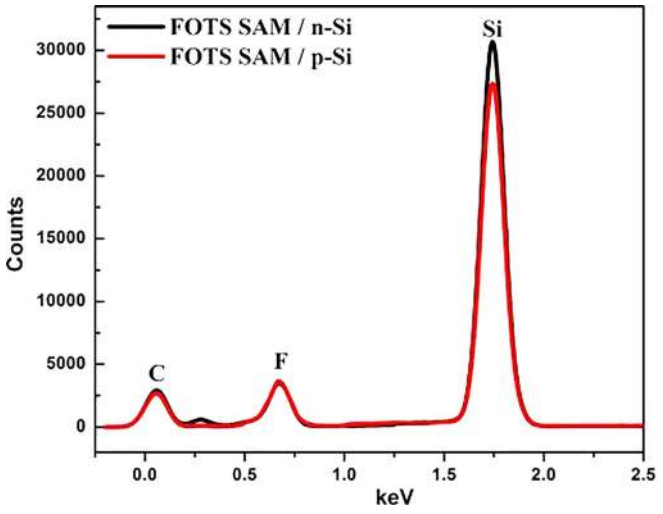

FIG. 4. EDAX Spectra of the FOTS SAM coated on n-Si and p-Si surfaces.

topographic measurement, we estimated that the rms roughness of the n-Si surface is about 1.5 nm and p-Si surface is about 1.9 nm. The topography images of n-Si and p-Si are shown in Figs. 5 and 6. The FOTS SAM coated p-Si surface (Fig. 5) is heterogeneous and has domains with different orientations. But the FOTS SAM coated n-Si surface is uniform and homogeneous. From the surface analysis, we observed that the FOTS SAM on n-Si surfaces is well ordered and homogeneous than that of the FOTS SAM on p-Si surfaces.

B. Flow-voltage measurements

Figure 7 shows the nitrogen gas flow induced voltage (V) generations of uncoated, half coated, and full coated n-Si wafers (immersed for 15 min, 2, and 18 h). From Figure 7, it is very clear that the voltage generated by the 2 and 18 h immersed samples of half coated and full coated n-Si wafers does not show significant variation from the 15 min immersed samples. For our geometry $\theta = \pi/4$, the temperature difference along the streamline in the gas flow will induce a temperature difference in the solid along the flow direction. The temperature difference, in turn, will result in a voltage difference V, defined as $V_L - V_R$, due to the Seebeck effect. We know that the Seebeck coefficient is positive for p-type (majority carriers are holes) and negative for n-type materials (majority carriers as electrons). From the results, it is observed that the flow induced voltage is proportional to the flow velocity, and the measured voltage generated by half coated and full coated n-Si wafers is higher than that of uncoated at given flow velocity. Moreover, the half coated n-Si generated higher voltages than those of full coated n-Si wafers at a given flow velocity.

Figure 8 shows that the nitrogen gas flow induced voltage (V) generations of uncoated, half coated, and full coated p-Si wafers (immersed for 15 min, 2 and 18 h). From Figure 8, it is very clear that the voltage generated by the 2 and 18 h immersed samples of half coated and full coated p-Si wafers does not show significant variation from the 15 min immersed samples. Similarly, it is observed that the flow induced voltage is proportional to the flow velocity, and the measured voltage generated by half coated and full coated p-Si wafers is higher than that of uncoated at given flow velocity. Moreover, the half coated p-Si generated higher voltages than those of full coated p-Si wafers at a given flow velocity. At the flow velocity of 26.52 ms^{-1}, the full coated n-Si generated 1.4 mV and half coated p-Si generated 2.17 mV, which is about 1.5 times that of full coated response voltage.

From the flow induced voltage measurements, from Figures 7 and 8, it is observed that the n-Si surfaces generate more voltage than that of the p-Si surface for a given flow velocity. Order/disorder and homogeneous/ heterogeneous assembly of the FOTS SAM on the n-Si and p-Si wafers play a major role in the voltage generation. The surface analysis by FTIR and AFM (Figures 3–6) clearly shows that the FOTS SAM on p-Si is disordered and heterogeneous that that of the n-Si surfaces. Therefore, the heterogeneity and disorder state of FOTS SAM directly influence the Seebeck coefficient and voltage generation due to changes in the electronic energy levels and band gap. For a comparison, the

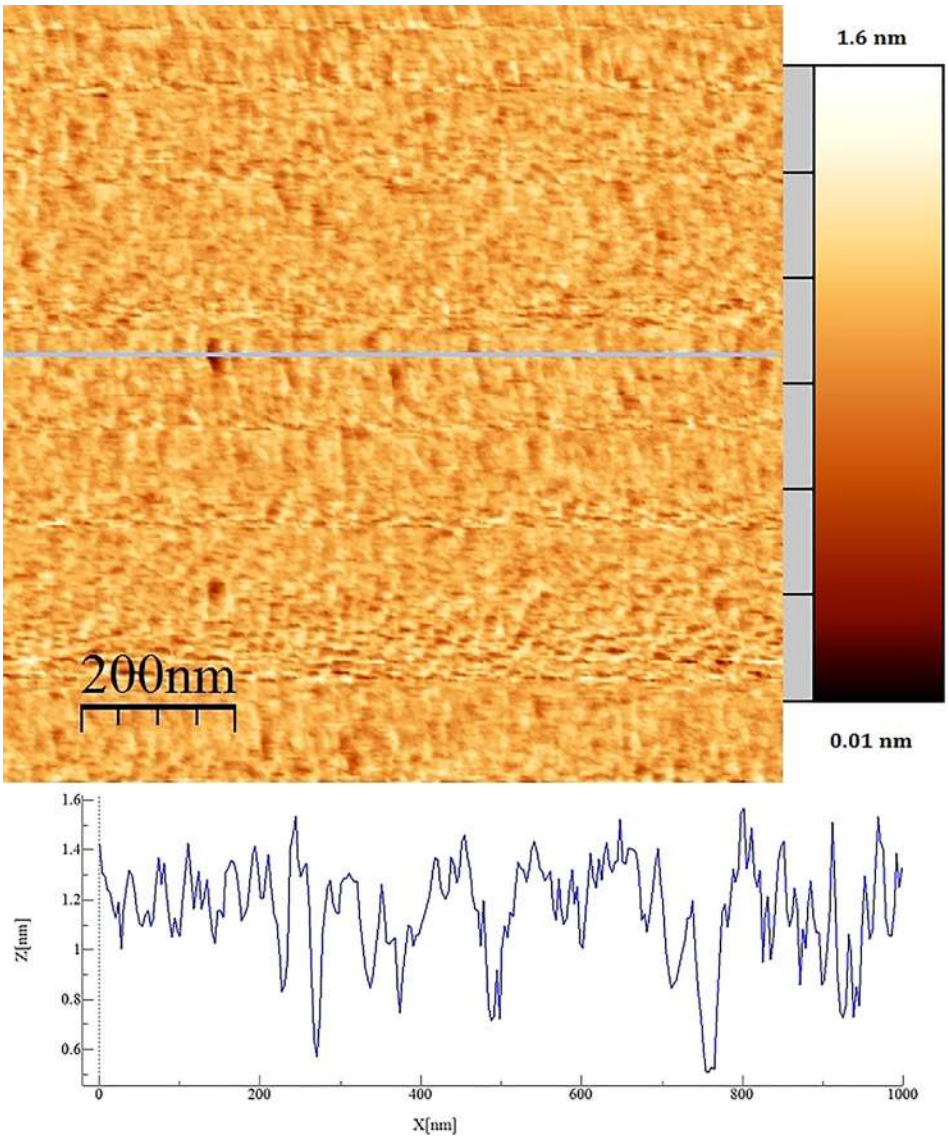

FIG. 5. AFM contact mode image of the FOTS SAM on the n-Si surface, and the line profile shows height variations in the z-direction.

estimated response voltages for the uncoated, full coated, and half coated n-Si and p-Si surfaces at the flow velocity of 26.52 ms^{-1} are given in Table I.

Figures 9 and 10 show the plots of flow induced voltage (V), over a range of values of u and u^2 of the uncoated, half coated, and full coated n-Si and p-Si. Analysing the flow induced voltage (V) versus velocity u, it is observed that there are two response regimes, (i) linear regime and (ii) parabolic regime. Figure 9 shows that the flow induced voltage V increases linearly with velocity below $u = 10\,ms^{-1}$ and increases parabolically above the velocity $u > 10\,ms^{-1}$ and up to $u < 26\,ms^{-1}$. Figure 10 shows voltage V versus square of the velocity u^2, and it clearly indicates the linearity between V and u^2 and V and M_n^2. Using Equations (8) and (9) and linear curve fitting of Figure 10, the respective proportionality constants D_s and A_s were estimated and the values are given in Table II.

In this research work, we successfully developed and studied highly sensitive nitrogen gas flow sensors. The effect of surface modification on the flow induced voltage generation of the n-Si and p-Si semiconductors was investigated. FOTS SAM modified highly doped n-Si and p-Si were very sensitive to flow of nitrogen gas. The nitrogen gas flow induced voltage measurements of the uncoated, full, and half coated n-Si and p-Si wafers (Figures 7 and 8) showed that the flow induced voltage generations increase parabolically with flow velocity, as expressed in Equations (7)–(9). It is also observed that (i) full coated n-Si and p-Si wafers generated more voltage than that of the uncoated and (ii) half coated (FOTS-SAM) n-Si, and p-Si generated more voltage than that of the full coated. Maximum voltages generated by the uncoated and coated n-Si and p-Si wafers at the flow velocity of 26.5 ms^{-1} are given in Table I. The flow induced voltage versus the velocity can be divided into two linear regimes (i) $u \leq 10\,ms^{-1}$; (ii) $u > 10\,ms^{-1}$ and up to $u < 26\,ms^{-1}$. The velocity sensitivities S_{u_1} and S_{u_2} of the two linear regimes of the uncoated and coated n-Si and p-Si wafers are given in Table III. The FOTS SAM surface modification of n-Si and p-Si wafers increased the sensitivities S_{u_1} and S_{u_2} significantly. Referring Equations (8) and (9) and Table II, the proportionality constants D_s and A_s increase linearly with square of the velocity (u^2) and Mach number (M_n^2). Therefore, the half coated n-Si and p-Si wafers are more sensitive to nitrogen gas flow than that of the full coated and the uncoated. This enhanced voltage generation

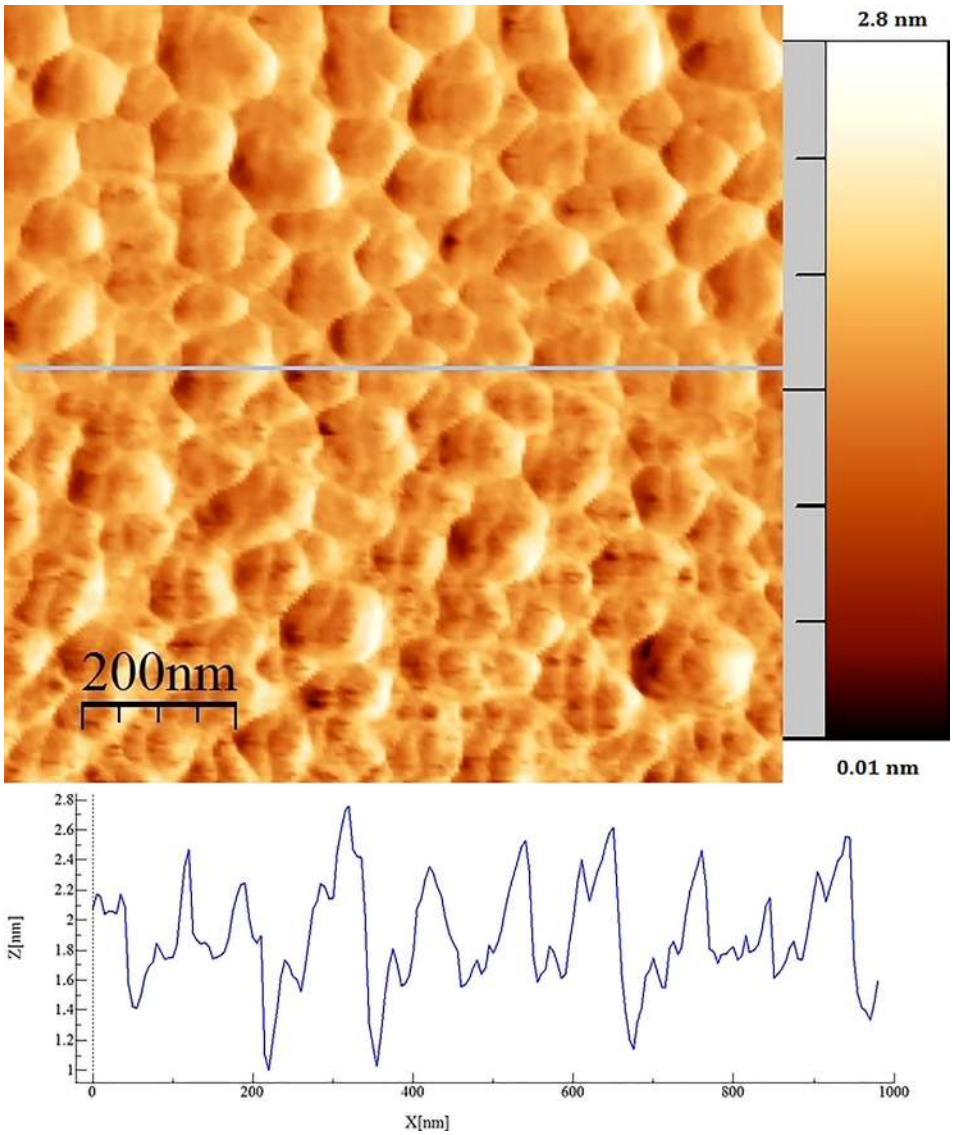

FIG. 6. AFM contact mode image of the FOTS SAM on the p-Si surface, and the line profile shows height variations in the z-direction.

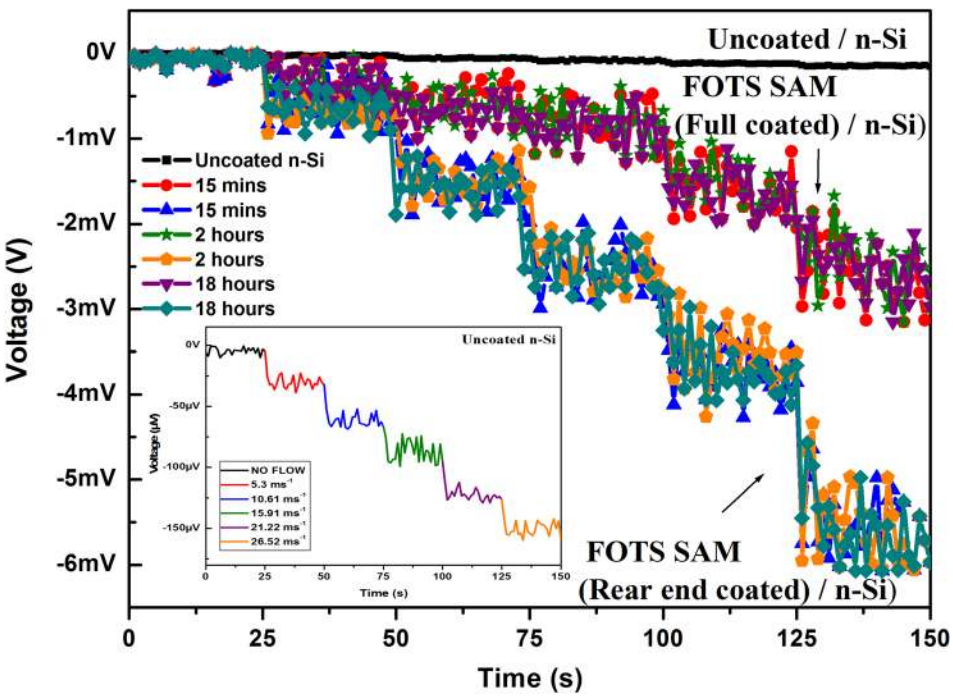

FIG. 7. Voltage generated by uncoated, full coated, and half coated n-Si sensors due to flow of nitrogen gas velocities at 0.0, 5.3, 10.61, 15.91, 21.22, and 26.52 ms^{-1}.

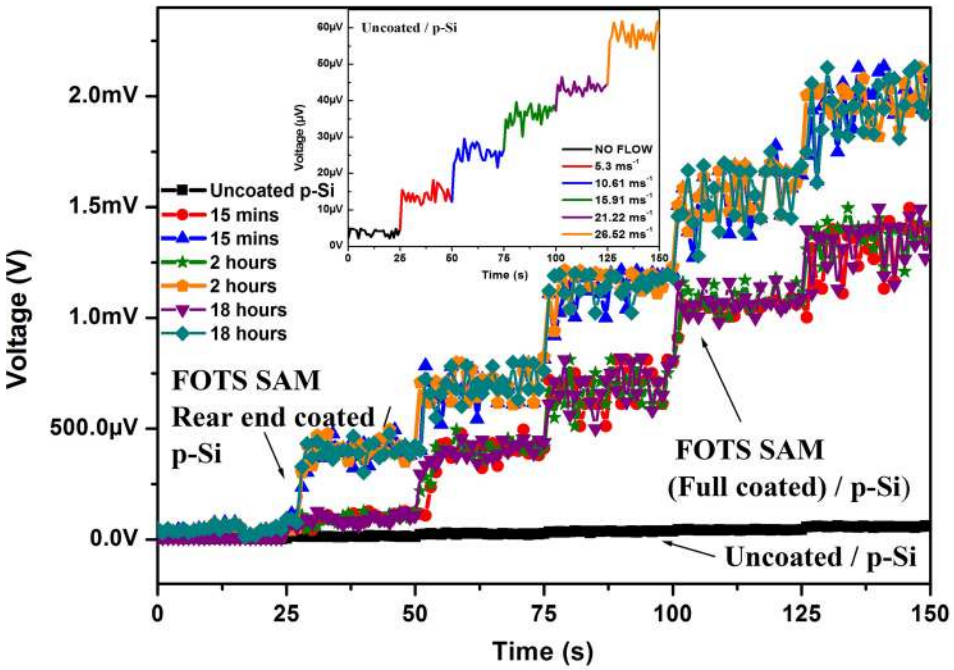

FIG. 8. Voltage generated by uncoated, full coated, and half coated p-Si sensor due to flow of nitrogen gas velocities at 0.0, 5.3, 10.61, 15.91, 21.22, and 26.52 ms^{-1}.

TABLE I. Voltage generated by FOTS SAM coated n-Si and p-Si sensors at 26.52 ms^{-1}.

Material type	Response voltage (mV)
Uncoated n-Si	-0.15 ± 0.01
Full coated n-Si	-3.15 ± 0.08
Half coated n-Si	-6.07 ± 0.33
Uncoated p-Si	0.06 ± 0.01
Full coated p-Si	1.41 ± 0.06
Half coated p-Si	2.13 ± 0.15

of the FOTS SAM modified n-Si and p-Si could be understood and explained by invoking the electronic Band Theory of Semiconductors.

Band theory based derivations and analysis of Seebeck coefficient (α_s) and inference of experimental results show that both the Seebeck coefficient and hence the flow induced

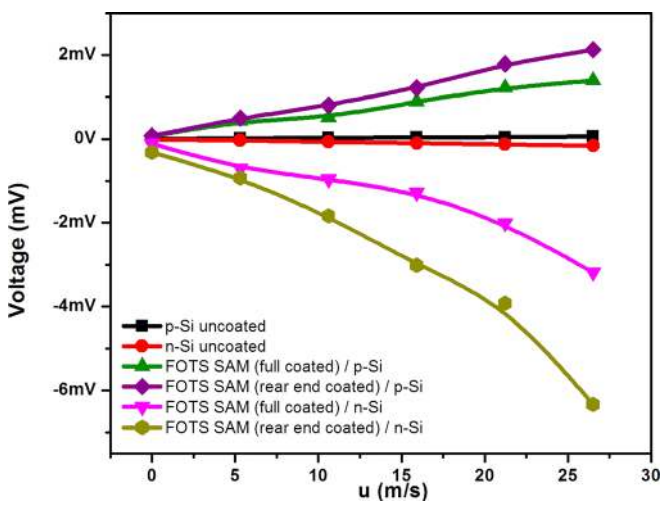

FIG. 9. Plot of voltage versus u (velocity) of FOTS SAM uncoated, half coated, and full coated n-Si and p-Si surfaces.

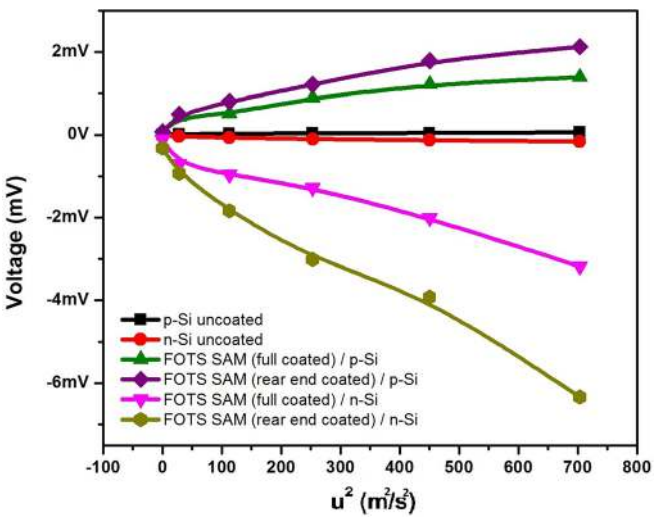

FIG. 10. Plot of voltage versus u^2 of FOTS SAM uncoated, half coated, and full coated n-Si and p-Si surfaces.

voltage generations of FOTS SAM-n-Si and p-Si interfaces were influenced by the changes in values of the Fermi Energy (E_F), conduction band energy level (E_c), valence band energy level (E_v), electrical conductivity (σ), energy barrier between FOTS SAM and n-Si, and phonon-electron momentum transfer, which result in trapping and

TABLE II. Constants D_s and A_s of FOTS SAM coated n-Si and p-Si wafers.

Material type	D_s ($\mu V\, s^2\, m^{-2}$)	A_s(V)
Uncoated n-Si	−0.22	−0.025
Full coated n-Si	−3.9	−0.48
Half coated n-Si	−8.1	−0.99
Uncoated p-Si	0.072	0.012
Full coated p-Si	1.8	0.221
Half coated p-Si	2.7	0.334

TABLE III. Velocity sensitivity $S_{u_1} \leq 10\,\mathrm{ms}^{-1}$ and $S_{u_2} > 10\,\mathrm{ms}^{-1}$ and $< 26\,\mathrm{ms}^{-1}$.

Sample type	$S_{u_1}(\mu\mathrm{V\,s\,m}^{-1})$	$S_{u_2}(\mu\mathrm{V\,s\,m}^{-1})$
Uncoated n-Si	−5.5	−5.7
Full coated n-Si	−81.1	−142.2
Half coated n-Si	−141.5	−273.1
Uncoated p-Si	2.3	2.0
Full coated p-Si	42.3	56.1
Half coated p-Si	69.2	85.4

accumulation of charge carriers at the interfaces. It is further observed that the synergism of different mechanisms contributes to the cumulative increase of flow induced voltage of the FOTS SAM modified surfaces. The enhanced voltage generations and high sensitivities are caused by an effective increase of the gradient of Fermi Energy (E_F) (Seebeck coefficient) due to FOTS SAM coatings and influenced by (i) the electron and hole density distributions, intrinsic band energy levels and band gap energy, formation of an electron-depletion layer (EDL) in n-type oxide semiconductors, hole-accumulation layer (HAL) in p-type oxide semiconductors; (ii) asymmetrical potential difference between the coated and uncoated regions; (iii) electrical and thermal conductivities and their transport characteristics on the surface and the subsurface; (iv) accumulation of charge carriers; (v) the molecular level interactions between nitrogen gas molecules and the perfluoro CF_3, CF_2, CF groups; (vi) degree of molecular order and orientation, conformational transitions, thermal stability, gradient *janus* (philic-phobic) interaction of the FOTS SAM.

This study showed that the FOTS SAM surface modified n-Si and p-Si wafers are very good candidates for nitrogen gas flow sensing and for energy harvesting applications. The outcomes of this work are promising and will open up new applications of organic-inorganic interfaces for specific gas sensing, energy harvesting, and detection of impurities in gas and the environment.

ACKNOWLEDGMENTS

The authors thank funding agency and affiliated institutions, DST-Nanomission, Government of India, Grant No: DST-Nanomission/SR/NM/PG-04-2008/25-02-2009, Karunya University, Coimbatore, VIT University, Chennai Campus, InCUBE-EngSciRes R&D, Udumalpet, Coimbatore, for providing financial support to carry out this research work. We also thank Mr. A. Raja and Mr. M.B.S. Praveen, lab technicians of the Centre for Research in Nanotechnology, KU, for their technical support. We are very grateful to Professor. M. S. Bobji and Professor Sathis Vasu Kailash, Department of Mechanical Engineering, Indian Institute of Science for the valuable discussions and suggestions. Finally, we thank Mr. Shama Sunder, Nanotribology Lab, Indian Institute of Science for the service and necessary technical help to carry out FTIR and AFM measurements.

[1]A. Ulman, "Formation and structure of self-assembled monolayers," Chem. Rev. **96**, 1533–1554 (1996).
[2]D. Devaprakasam, S. Sampath, and S. K. Biswas, "Thermal stability of perfluoroalkyl silane self-assembled on a polycrystalline aluminum surface," Langmuir **20**, 1329–1334 (2004).
[3]B. C. Bunker, R. W. Carpick, R. A. Assink, M. L. Thomas, M. G. Hankins, J. A. Voigt, D. Sipola, M. P. de Boer, and G. L. Gulley, "The impact of solution agglomeration on the deposition of self-assembled monolayers," Langmuir **16**, 7742–7751 (2000).
[4]O. P. Khatri and S. Biswas, "Thermal stability of octadecyltrichlorosilane self-assembled on a polycrystalline aluminium surface," Surf. Sci. **572**, 228–238 (2004).
[5]J. Christopher Love, J. K. Kriebel, R. G. Nazzo, L. A. Estroff, and G. M. Whitesides, "Self-assembled monolayers of thiolates on metals as a form of nanotechnology," Chem. Rev. **105**, 1103–1170 (2005).
[6]S. Onclin, B. J. Ravoo, and D. N. Reinhoudt, "Engineering silicon oxide surfaces using self-assembled monolayers," Angew. Chem., Int. Ed. **44**, 6282–6304 (2005).
[7]D. Devaprakasam and S. K. Biswas, "Molecular damping: Mechanical response of self-assembled monomolecular layer to compression," Phys. Rev. B **72**, 125434 (2005).
[8]D. Devaprakasam and S. K. Biswas, "Measurement of stiffness and damping constant of self-assembled monolayers," Rev. Sci. Instrum. **76**, 035102 (2005).
[9]T. M. Mayer, M. P. de Boer, N. D. Shinn, P. J. Clews, and T. A. Michalske, "Chemical vapor deposition of fluoroalkylsilane monolayer films for adhesion control in microelectromechanical systems," J. Vac. Sci. Technol., B **18**, 2433–2440 (2000).
[10]T. V. Desai, A. R. Woll, F. Schreiber, and J. R. Engstrom, "Nucleation and growth of perfluoropentacene on self-assembled monolayers: Significant changes in island density and shape with surface termination," J. Phys. Chem. C **114**, 20120–20129 (2010).
[11]H. Ahn and J. E. Whitten, "Vapor-deposition of aluminum on thiophene-terminated self-assembled monolayers on gold," J. Phys. Chem. B **107**, 6565–6572 (2003).
[12]Y. X. Zhuang, O. Hansen, T. Knieling, C. Wang, P. Rombach, W. Lang, W. Benecke, M. Kehlenbeck, and J. Koblitz, "Thermal stability of vapor phase deposited self-assembled monolayers for MEMS anti-stiction," J. Micromech. Microeng. **16**, 2259 (2006).
[13]Y. X. Zhuang, O. Hansen, T. Knieling, C. Wang, P. Rombach, W. Lang, W. Benecke, M. Kehlenbeck, and J. Koblitz, "Vapor-phase self-assembled monolayers for anti-stiction applications in MEMS," J. Microelectromech. Syst. **16**, 1451–1460 (2007).
[14]S. Allison, R. Smith, D. Howard, C. Gonzlez, and S. Collins, "A bulk micromachined silicon thermopile with high sensitivity," Sens. Actuators, A **104**, 32–39 (2003).
[15]D. Aswal, S. Lenfant, D. Guerin, J. V. Yakhmi, and D. Vuillaume, "Self assembled monolayers on silicon for molecular electronics," Anal. Chim. Acta **568**, 84–108 (2006).
[16]T. H. Geballe and G. W. Hull, "Seebeck effect in silicon," Phys. Rev. **98**, 940–947 (1955).
[17]A. V. Herwaarden, "The seebeck effect in silicon ICs," Sens. Actuators **6**, 245–254 (1984).
[18]A. V. Herwaarden and P. Sarro, "Thermal sensors based on the seebeck effect," Sens., Actuators **10**, 321–346 (1986).
[19]C. Herring, "Theory of the thermoelectric power of semiconductors," Phys. Rev. **96**, 1163–1187 (1954).
[20]S. Ghosh, A. Sood, and N. Kumar, "Carbon nanotube flow sensors," Science **299**, 1042–1044 (2003).
[21]A. K. Sood and S. Ghosh, "Direct generation of a voltage and current by gas flow over carbon nanotubes and semiconductors," Phys. Rev. Lett. **93**, 086601 (2004).
[22]S. S. Sarkar, S. Ghosh, and A. Sood, "Response time measurement in flow induced signal generation on semiconductors," Sens. Actuators, A **137**, 209–212 (2007).
[23]S. Ghosh, A. K. Sood, S. Ramaswamy, and N. Kumar, "Flow-induced voltage and current generation in carbon nanotubes," Phys. Rev. B **70**, 205423 (2004).
[24]A. Sood, "Carbon nanotubes: Pressure-induced transformations and voltage generation by flow of liquids," Radiat. Phys. Chem. **70**, 647–653 (2004).
[25]A. Sood, S. Ghosh, and N. Kumar, "Flow driven electronic transport in carbon nanotubes," Int. J. Nanosci. **4**, 839–848 (2005).
[26]A. Sood, S. Ghosh, and A. Das, "Flow-driven voltage generation in carbon nanotubes," Pramana **65**, 571–579 (2005).

[27]J. Yin, Z. Zhang, X. Li, J. Zhou, and W. Guo, "Harvesting energy from water flow over graphene," Nano Lett. **12**, 1736–1741 (2012).
[28]P. Dhiman, F. Yavari, X. Mi, H. Gullapalli, Y. Shi, P. M. Ajayan, and N. Koratkar, "Harvesting energy from water flow over graphene," Nano Lett. **11**, 3123–3127 (2011).
[29]J. Liu, L. Dai, and J. W. Baur, "Multiwalled carbon nanotubes for flow-induced voltage generation," J. Appl. Phys. **101**, 064312 (2007).
[30]P. Král and M. Shapiro, "Nanotube electron drag in flowing liquids," Phys. Rev. Lett. **86**, 131–134 (2001).
[31]L. D. Landau and E. M. Lifshitz, in *Fluid Mechanics*, 2nd ed. (Butterworth/ Heinemann, Washington, DC/London, 1998), p. 319.
[32]L. D. Landau and E. M. Lifshitz, in *Physical Kinetics*, 2nd ed. (Butterworth/ Heinemann, Washington, DC/London, 1998), p. 51.
[33]M. Asheghi, K. Kurabayashi, R. Kasnavi, and K. E. Goodson, "Thermal conduction in doped single-crystal silicon films," J. Appl. Phys. **91**, 5079–5088 (2002).